

Lab on a Chip

Devices and applications at the micro- and nanoscale

Accepted Manuscript

This article can be cited before page numbers have been issued, to do this please use: Y. Zhang, X. Fu, W. Guo, Y. Deng, B. Binks and H. C. Shum, *Lab Chip*, 2019, DOI: 10.1039/C9LC00722A.



This is an Accepted Manuscript, which has been through the Royal Society of Chemistry peer review process and has been accepted for publication.

Accepted Manuscripts are published online shortly after acceptance, before technical editing, formatting and proof reading. Using this free service, authors can make their results available to the community, in citable form, before we publish the edited article. We will replace this Accepted Manuscript with the edited and formatted Advance Article as soon as it is available.

You can find more information about Accepted Manuscripts in the [Information for Authors](#).

Please note that technical editing may introduce minor changes to the text and/or graphics, which may alter content. The journal's standard [Terms & Conditions](#) and the [Ethical guidelines](#) still apply. In no event shall the Royal Society of Chemistry be held responsible for any errors or omissions in this Accepted Manuscript or any consequences arising from the use of any information it contains.

ARTICLE

Electrocoalescence of Liquid Marbles driven by Embedded Electrodes for Triggered Bio-reaction†

Yage Zhang,^{a,b} Xiangyu Fu,^{a,b} Wei Guo,^{a,b} Yi Deng,^{a,c} Bernard P. Binks^d and Ho Cheung Shum^{a,b,*}Received 00th January 20xx,
Accepted 00th January 20xx

DOI: 10.1039/x0xx00000x

Liquid marbles need to be controlled precisely to benefit applications, for instance, as micro-reactors on digital microfluidics platforms for chemical and biological assays. In this work, a strategy is introduced to coalesce liquid marbles *via* electrostatics, where two contacting liquid marbles can coalesce when a sufficiently high voltage is applied to the embedded electrodes. With the understanding of the mechanism of coalescence through relating the electric stress and the restoring capillary pressure at the contacting interface, this method coalesces liquid marbles efficiently. When compared with the existing electrocoalescence method, our approach does not require immersion of the electrodes to trigger coalescence. We demonstrate this to exchange the medium for the culture of cell spheroids and to measure cell metabolic activity through a CCK-8 assay. The manipulation of liquid marbles driven by electrostatics creates new opportunities to conduct chemical reactions and biomedical assays in these novel micro-reactors.

1. Introduction

Liquid droplets have been investigated as discrete and digitized micro-reactors in microfluidics-based applications to achieve low-cost and high-throughput detections.^{1, 2} However, bare droplets tend to wet the contacting substrate and lead to carry-over and cross-contamination.³ An approach to eliminate wetting is to coat droplets with nano-/micro-sized hydrophobic particles, often known as liquid marbles.⁴ Compared with bare droplets, the liquid content in the liquid marbles does not contact directly with external substrates, hence free of cross-contamination, and the particle layer also enhances marble robustness and reduces evaporation.⁵⁻⁷ Coating particles that encapsulate the liquid droplet not only stabilize the liquid-air interface, but also catalyse the subsequent biological or chemical reactions.⁸⁻¹¹ Liquid marbles have also been applied for blood typing,¹² water pollution detection,¹³ gas sensing^{14, 15}, drug delivery^{16, 17} and culture of tumour and cell spheroids.¹⁸⁻²¹

Despite the promise of liquid marbles as micro-reactors on digital microfluidic platforms, their applications require exquisite control of multiple marbles. To this end, various methods have been applied to coalesce liquid marbles controllably by introducing external fields, including gravitational, acoustic and magnetic.²² For example, vertical

collision of liquid marbles has been found to induce their coalescence upon impact;^{23, 24} or by accelerating liquid marbles *via* rolling to gain kinetic energy.²⁵ Liquid marbles can also be manipulated to coalesce *via* acoustic levitation.^{26, 27} However, these approaches require complex peripheral instruments such as a high voltage converter and acoustic levitator, as well as tedious manual work. Hydrophobic magnetic particles have also been used to control the coalescence of liquid marbles,²⁸⁻³¹ though it is only limited to marbles coated with magnetic particles. Alternatively, liquid marbles can be induced to coalesce *via* electrostatics. For instance, two liquid marbles can be coalesced by applying a DC voltage through electrodes that are directly immersed in them.^{32, 33} The electrocoalescence of marbles is robust and controllable, but the direct contact of the electrodes with different marbles can result in cross-contamination and destabilization of marble micro-reactors. Furthermore, electrolysis can be triggered and limit the applicability of the method (Figure S1a).³³ Therefore, a robust and general electrocoalescence approach for marble micro-reactors without immersion of electrodes is urgently needed.

In this work, we propose a facile strategy to coalesce liquid marbles with non-immersed electrodes by embedding electrode plates under a layer of dielectric. This approach can avoid the problem of severe electrolysis, even if the coalesced marble is charged with a high voltage for several minutes after coalescence (Figure S1b). This approach is general for coalescing liquid marbles coated with particle sizes ranging from hundreds of nanometers to a few tens of micrometers. While marbles coated with micron-sized particles are deformed during coalescence, nanoparticle-coated marbles retain their spherical shape. As the maintenance of shape can facilitate further marble manipulation, we focus on nanoparticle-coated liquid marbles in this work. The electrocoalescence of these marbles occurs only above a critical voltage. The critical voltage depends significantly on the size of the stabilizing particles, the surface tension of the encapsulated liquid and the thickness of the

^a Department of Mechanical Engineering, University of Hong Kong, Pokfulam Road, Hong Kong.

^b HKU-Shenzhen Institute of Research and Innovation (HKU-SIRI), Shenzhen, Guangdong, 518057, China.

^c School of Chemical Engineering, Sichuan University, Chengdu, 610065, China.

^d Department of Chemistry and Biochemistry, University of Hull, Hull, HU6 7RX, UK.

† Electronic Supplementary Information (ESI) available: (1) Correlation between the theoretical critical voltage and various physical parameters. (2) Sample videos for liquid marbles coated with particles of different sizes are available. See DOI: 10.1039/x0xx00000x

dielectric. The dependence can be explained by balancing the electric stress and capillary pressure. Moreover, the electrical conductivity of the aqueous droplet also affects the critical voltage. This effect is attributed to the non-negligible electric double-layer capacitance induced in nanoparticle-coated liquid marbles. Finally, we perform an assay of cell metabolic activity based on this approach, highlighting its potential for biomedical analysis.

2. Experimental Section

2.1. Materials

Liquid marbles were prepared by depositing aqueous droplets on a hydrophobic particle bed. Coating particles included PTFE grains (diameter = 35 μm , particle-water contact angle = 110°, Sigma-Aldrich, USA), silicone resin particles (diameter = 2.0 μm , 6.0 μm or 12.0 μm , particle-water contact angle = 91°, Momentive Performance Material Inc., Japan), silicone particles (diameter = 5.0 μm , NanoMicro Tech. Inc., China) as well as silica nanoparticles (primary diameter 7 nm, particle-water contact angle = 118°, Aerosil R812, Evonik, Germany). Deionized (DI) water (Direct-Q, Merck Millipore, Germany) was used for most experiments, unless otherwise stated. The surface tension of the liquid phase γ was varied by dissolving sodium dodecyl sulfate (Aladdin, China) in DI water at different concentrations. The values of the surface tension were measured using the pendant-drop method.^{34,35} The viscosity of the liquid η was changed by dissolving dextran (Pharmacosmos, Denmark) in DI water at different weight fractions, and the value was measured using a microfluidic viscometer (microVISC, Rheosense Inc.). Sodium chloride (99.5%, Sigma-Aldrich) was added to DI water at different concentrations to vary the electrical conductivity κ of the liquid, and the conductivity was measured by an electrical conductivity meter (CyberScan COND 610, Eutech Inc). The dielectric layer was prepared by mixing poly(dimethylsiloxane) (PDMS) and curing agent (Dow Corning, USA) at a weight ratio of 10:1. The thickness of the dielectric layer was manipulated by adjusting the rotation speed of the spin coater (WS-650MZ-23NPPB, Laurell) and measured by a profilometer (DektakXT, Bruker). Human bone marrow-derived mesenchymal stem cells (hBMSCs) were purchased from American Type Culture Collection (ATCC, PCS-500-012, VA, USA). Dulbecco's modified Eagle medium (DMEM), hanks' balanced salt solution (HBSS), fetal bovine serum (FBS), 0.25% Trypsin-EDTA, 100x penicillin and streptomycin were purchased from Gibco (Grand Island, NY, USA). We prepared the culture medium by adding 10% (v/v) FBS, 1% (v/v) penicillin and streptomycin into fresh DMEM. The cell counting kit-8 (CCK-8) was bought from KeyGEN BioTECH, China. Centrifugation was performed in a Thermo Scientific Sorvall ST 8R Centrifuge, adapted with a HIGHConic III rotor.

2.2. Experimental Setup

The setup for electrocoalescence of liquid marbles comprised a lifting platform, an open-sourced printed circuit board (PCB) design which incorporated embedded electrodes covered by a PDMS dielectric layer, a high-voltage supply, a LED lamp, a high-speed camera and a computer monitor (Figure 1a). Two neighbouring electrodes on the open-source digital microfluidics design (OpenDrop V2, Gaudi Lab) were applied as embedded electrodes, and the whole design was fabricated by common PCB protocols. A dielectric layer made of PDMS was deposited on top of the electrodes, and two metal wires were soldered to the two selected electrodes at the backside of the

PCB. The PCB board was fixed to a lifting platform using double-sided tape. The high DC voltage supply was then connected to the electrodes. A high-speed camera (Photron Fastcam SA3) was used to record the side view of the coalescence of liquid marbles. Recorded videos and images were viewed by the camera software Photron Fastcam Viewer (PFV) and then analyzed using ImageJ (National Institutes of Health, USA).

2.3. Preparation of liquid marbles

To prepare liquid marbles, a pipette (Eppendorf Research plus) was used to deposit liquid droplets onto a plastic culture dish covered by a layer of nano- or micro-sized particles. The volume V_{ol} of the liquid marble for test (unless otherwise stated) was 10 μL . Slight tilting and gentle rolling of the dish caused the droplet to become coated with particles. After formation, two liquid marbles were transported to the platform from the particle bed using a plastic spoon. Liquid marbles were placed on top of two adjacent electrodes and pushed to contact with each other using a rod treated by hydrophobic silane for the coalescence experiment.

2.4. Electrocoalescence of liquid marbles driven by embedded electrodes

Two metal wires were soldered to connect the embedded electrodes to the DC voltage supply (Tianjin Dongwen, China). The voltage was increased gradually until two liquid marbles coalesced. In the meantime, the high-speed camera recorded the lateral-view morphology of the liquid marbles at a frame rate of 3600 fps (unless otherwise stated). All experiments described were performed at room temperature (~ 25 °C) and relative humidity of 55%. Experiments were repeated at least 15 times to determine the average critical voltage.

2.5. Cell-contained liquid marble preparation and stem cell spheroids culturing in micro-reactors

hBMSCs were cultured in a common cell culture dish. When hBMSCs were cultured to 70-80% confluency, the cells were washed with HBSS buffer saline and dispersed into single cells by injecting 3 mL of 0.25% Trypsin and incubating for 3 min. 3 mL of DMEM medium was then injected into the culture dish to neutralize the Trypsin. After centrifuging the collected medium with suspended cells at 1,500 rpm/301.9 $\times g$ for 4 min, the supernatant was sucked out and replaced with fresh DMEM basal medium. Liquid marbles with a volume of 50 μL containing suspended cells at a density of 150/ μL were then fabricated by applying the liquid marble preparation method described above, and cultured in a humidified, 5% CO_2 atmosphere at 37 °C. A 10 μL liquid marble containing DMEM was merged into the liquid marble micro-reactors *via* electrocoalescence every other day to provide cells with adequate nutrition.

2.5. Bioapplications in liquid marbles triggered by electrocoalescence

CCK-8 assay was done on days 1, 3 and 5 of incubation, triggered by coalescing the cell-contained liquid marble with another 10 μL liquid marble containing CCK-8 reagents (Keygen Biotech, China). The marble after coalescence was then incubated inside a 1.5 mL centrifugal tube in a humidified, 5% CO_2 atmosphere at 37 °C for 3 h. Digital photographs of the liquid marbles were captured before coalescence, right after coalescence and after 3 h of incubation. Quantitative CCK-8 assay was performed by transferring 50 μL of coloured mixture from liquid marble micro-reactors into a well of a 96-well microplate. Another 50 μL DMEM medium was then injected into each well for dilution, resulting in a final volume of 100 μL per

well. The intensity of the solution was measured by a microplate reader (SpectraMax iD3, Molecular Devices), based on a colorimetric method with an excitation wavelength of 450 nm. A control group was conducted to culture hBMSCs inside a 96-well microplate, and a background which was bulk DMEM medium was introduced when hBMSCs are cultured in silica nanoparticle-based liquid marble micro-reactors.

3. Results and Discussion

3.1. Electrocoalescence of liquid marbles

In our approach, two liquid marbles are placed in contact with each other on a dielectric, with two adjacent electrode plates embedded beneath them (Figure 1b). Hydrophobic particle shells separate encapsulated liquid droplets and prevent coalescence when no voltage is applied, as shown in Figure 1c at 0 s. We gradually increase the DC voltage applied to the embedded electrodes until coalescence occurs. We increase DC voltage manually at an average rate of 20 volts per second. The ramp rate has been shown to demonstrate a limited effect on the critical voltage (Table S1). When the applied voltage is small, two liquid marbles attract each other as encapsulated droplets tend to merger under polarization. Their contacting interface flattens but does not lead to coalesce, due to the elasticity of the particle shell (Figure 1c, 21.894 s). Once the voltage applied exceeds a critical value U_c , coalescence is initiated at the contacting interface, indicated by the sudden expansion and continuous widening of the liquid bridge (Figure 1c, 21.900 s). Finally, the liquid bridge stops expanding and liquid marbles merge into a dumb-bell-shaped marble shown in Figure 1c, 22.000 s. The coalescence takes place within around 100 ms. Based on our experiments, electrocoalescence takes place only when the voltage reaches U_c . Holding a voltage below U_c for a longer period of time does not lead to coalescence.

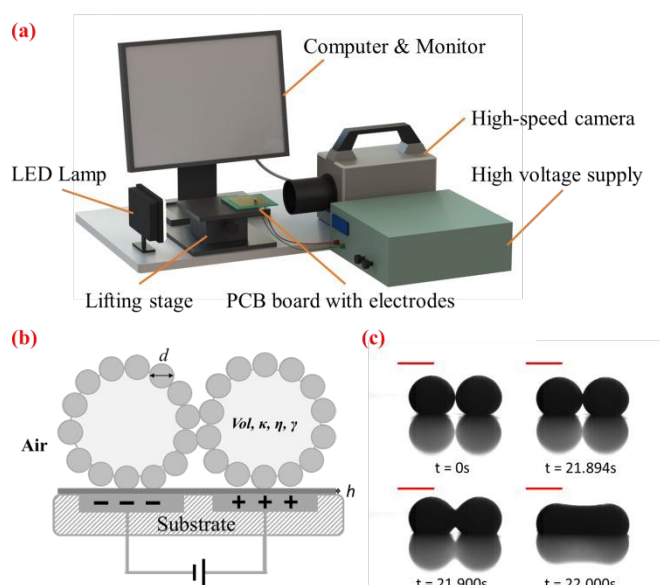


Figure 1. (a) Experimental setup for electrocoalescence of liquid marbles driven by embedded electrodes. (b) Schematic of the coalescence of two liquid marbles on a dielectric layer, with embedded electrodes charged through a high voltage supply. Vol , κ , η , and γ refer to the volume, electrical conductivity, viscosity and surface tension of the encapsulated liquid droplets respectively; d is the diameter of the hydrophobic stabilizing particles and h is the thickness of the dielectric

layer. (c) Evolution of morphology of liquid marbles under electrocoalescence. In this example, both liquid marbles before coalescence are formed by encapsulating 10 μ L DI water with 5 μ m black silicone particles. Voltage applied to embedded electrodes was set initially at 0 V and coalescence occurs when the voltage reached 400 V; scale bars = 2 mm.

We have applied this approach to liquid marbles covered by particles of various sizes shown in Table S2. This immersion-free electro-driven approach can induce coalescence not only for microparticle-coated liquid marbles but also for nanoparticle-coated ones. The versatility of this approach with respect to the particle size is highlighted and cannot be matched by the previous electrostatics-driven method.

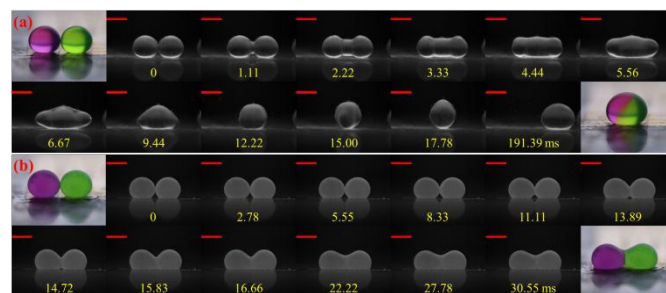


Figure 2. Two liquid marbles (10 μ L) coated with (a) R812 silica nanoparticles and (b) 6 μ m silicone resin particles, coalesced and merged into one large marble by increasing the voltage. The time immediately before formation of the liquid bridge is set as 0 ms. The coalescence of liquid marbles is indicated by the expansion of the liquid bridge. All experiments were performed with a dielectric layer thickness of 39 μ m. Scale bars = 2 mm. Inset color images were captured with a digital camera, while gray-scale images were shot using a high-speed camera.

In the immersion-free electrocoalescence of liquid marbles, the shape of the liquid marble after coalescence varies with the size of the coating particles. We selected liquid marbles coated with nano-/microparticles but which possess similar effective surface tension (illustrated in Figure S2 and Table S3). The coalescence of nanoparticle-coated marble is very similar to that of bare droplets, where the Laplace pressure gradient governs the fluid exchange by reducing the interfacial area and ends up with a merged marble with a quasi-spherical shape (Figure 2a).^{36, 37} During the collision, excess nanoparticles are found to detach from the liquid interface (Video S1). However, such a phenomenon is seldom observed for electrocoalescence of liquid marbles coated with microparticles on this platform. Two microparticle-coated liquid marbles coalesce into a dumb-bell-shaped marble (Figure 2b), with visible particles jamming at the neck region of the merged marble (Video S2). This can be attributed to the strong desorption energy of these particles, which is $\sim 2 \times 10^9$ kT from the air-water interface ($E = \pi R_{particle}^2 \gamma (1 \pm \cos \theta)^2$, $\gamma = 73$ mN m^{-1}) for a 6 μ m silicone resin particle with contact angle of 91°, which is three to four orders of magnitude larger than that for the nanoparticles.³⁸

The shape difference becomes more distinct when multiple liquid marbles are coalesced, as shown in Figure S3. Regardless of the number of liquid marbles before coalescence, nanoparticle-coated liquid marbles always merge into one spherical marble. For microparticle-coated liquid marbles, the shape after coalescence becomes more irregular with multiple particle jammed regions. The jammed particles lead to a loss of interfacial mobility of the merged liquid marble, hampering further manipulation. Among all types of

particles, the ability to maintain their shape after coalescence renders nanoparticle-coated liquid marbles easily manipulated using this electro-driven approach.

3.2. Influence of different physical parameters on the critical coalescence voltage U_c

We select nanoparticle-coated liquid marbles to investigate the influence of different parameters on electrocoalescence. We first change the volume Vol and the viscosity η of the interior droplet. For liquid marbles with droplet volume ranging from 5 μL to 20 μL (Figure 3a), the critical voltage U_c remains roughly constant. By modulating the concentration of dextran dissolved in water from 1 wt.% to 20 wt.%, the viscosity changes from 1.82 mPa s to 80.24 mPa s; nonetheless, the critical voltage U_c stays roughly the same (Figure 3b).

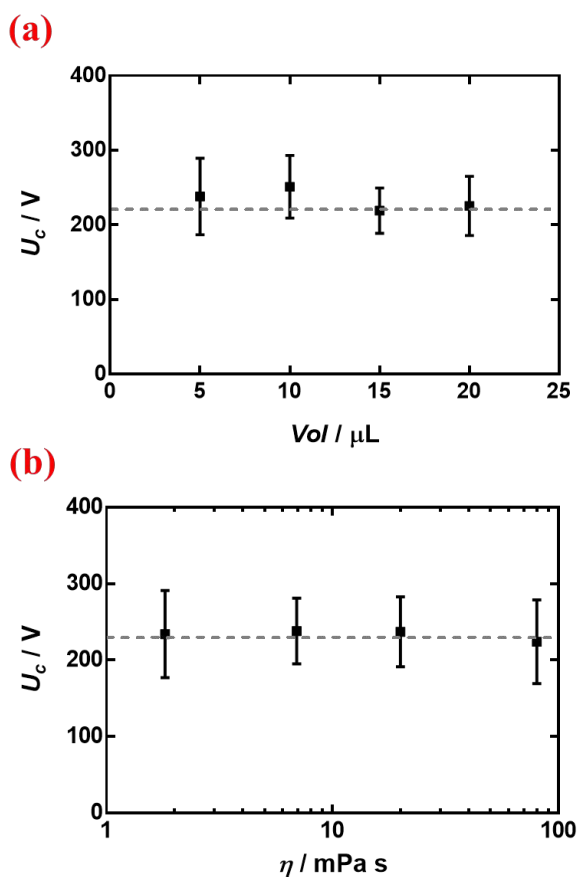
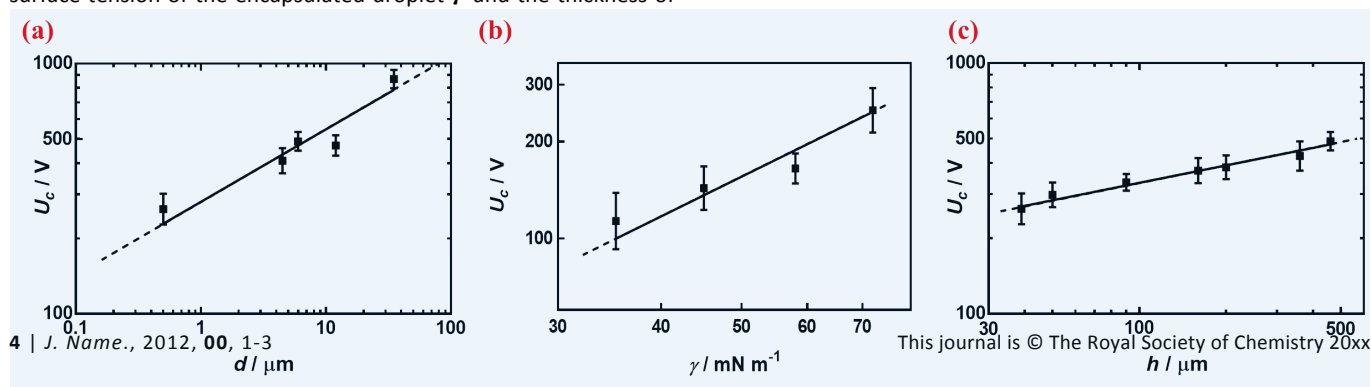


Figure 3. Variation of critical voltage U_c with (a) volume Vol of liquid marble and (b) viscosity η of the encapsulated droplet. Liquid marbles were coated with R812 silica nanoparticles.

We further demonstrate however that the critical voltage U_c depends significantly on the diameter of the coating particles d , the surface tension of the encapsulated droplet γ and the thickness of

the dielectric layer h . We notice that other than particle size d , materials with different properties may affect the electrical response, such as dielectric constant and particle shape.³⁹ To be specific, we measure the critical voltage U_c of liquid marbles coated with silica, silicone resin and PTFE particles of various sizes while similar surface tension is maintained. Both silica, silicone resin and PTFE have dielectric constants within the range of 2.1 to 5.0; and all particles are spherical. The result indicates that U_c increases significantly when the particle diameter d increases, as shown in Figure 4a. The surface tension γ of the encapsulated droplet is changed by adding SDS surfactant from 0.001 M to 0.008 M in 0.1M NaCl aqueous solution. The electrical conductivity of the 0.1M NaCl aqueous droplet is kept in the range of 761.0 $\mu\text{S cm}^{-1}$ to 786.6 $\mu\text{S cm}^{-1}$ by adding SDS of different concentration, while surface tension is declined from 75.45 mN m^{-1} to 35.24 mN m^{-1} . Thus, surface tension γ is considered the only variable in this set of experiments. Liquid marbles tend to coalesce more readily at lower surface tension (Figure 4b). The critical voltage U_c also depends on the thickness of the dielectric layer h ; an increase in h leads to an increase in U_c (Figure 4c).

As the droplet content is electrically conductive, we assume there is no voltage drop inside the droplet. We then construct a physical model to explain the dependence of the critical voltage U_c on the physical quantities. Referring to recent studies in the electrostatics-driven coalescence of Pickering emulsions⁴⁰ and liquid marbles,³² we analyze the stresses applied on the interface where two liquid marbles are in contact. When a voltage difference is applied across the embedded electrodes, the encapsulated droplets become polarized and exert local charge. The local charge would induce electric stress $\tau_E \sim \epsilon_0 \epsilon_r E_{loc}^2$ towards the opposing liquid interface, where $\epsilon_0 \epsilon_r$ is the relative permittivity of air and E_{loc} is the local electric field strength. The opposing interface will be deformed accordingly, followed by the formation of a conical tip from defects that exist on the interface with the size of L . The capillary pressure $\tau_S \sim \frac{\gamma}{L}$ resists the tip formation due to surface tension effects. Liquid marbles are expected to coalesce only when the applied voltage reaches a critical value and exerts sufficient electric stress to overcome the capillary pressure. To confirm this, we plot Figure 4e by calculating the electrical stress τ_E as y-axis and the capillary pressure τ_S as x-axis for all systems in Figures 4a-c (the derivation of E_{loc} is shown in Supporting Information). Previous work on Pickering emulsions indicates that coalescence would occur when defects at the interface have sizes similar to the particle diameter.⁴⁰ Defects with sizes of the same scale as particles can also be appreciated in Figure S4. Therefore, by approximating $L \sim d$, the capillary pressure can be evaluated from $\tau_S \sim \frac{\gamma}{d}$. We further derive a theoretical voltage U_{theory} that leads to coalescence of liquid marbles based on our model (derivation can be found in Supporting Information). The result has been plotted against the experimental data in Figure 4f. The excellent agreement confirms that coalescence is triggered by liquid interface deformation driven by electrostatics.



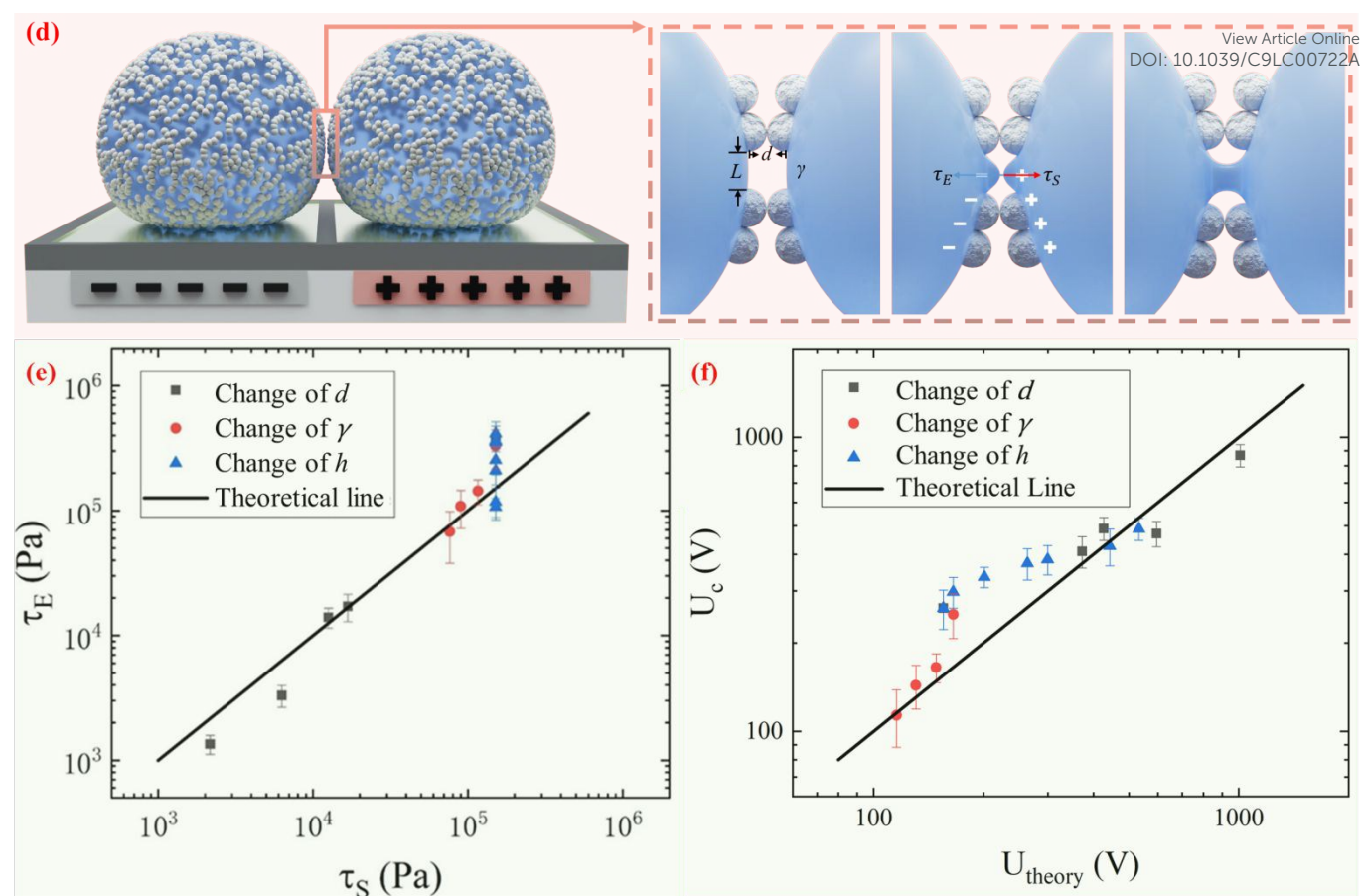


Figure 4. (a) Log-log plot showing the dependence of critical voltage U_c on particle diameter d . (b) Log-log plot demonstrating the response of critical voltage towards surface tension γ of the liquid droplet. (c) Log-log plot demonstrating the influence of dielectric layer thickness h on the critical value U_c . All liquid marbles were coated with R812 silica nanoparticles except in (a), where different types of particle were used to vary the diameter. (d) Schematic showing the process of a typical electrocoalescence which occurs when the electric stress acting on the particle-stabilized interface and the restoring capillary pressure are no longer balanced. Tips formed from defects on the particle-stabilized interface and the formation of a liquid bridge initiate the coalescence. (e) Log-log plot of the electric stress $\tau_E \sim \epsilon_0 \epsilon_r E_{Loc}^2$ versus the capillary pressure $\tau_S \sim \frac{\gamma}{d}$ for all conditions in (a) - (c). The theoretical line has a slope of unity. (f) Comparison of the theoretical value of U_c with the experimental one.

Other than physical quantities directly affecting stresses, U_c also depends on the electrical conductivity κ of the encapsulated droplet. The conductivity changes from $0.070 \mu\text{S cm}^{-1}$ to $29,500 \mu\text{S cm}^{-1}$ when the concentration of sodium chloride dissolved in deionized water is changed from 0 M to 5 M. By increasing the electrical conductivity κ of the encapsulated electrolytic droplet, a lower voltage is needed to trigger the coalescence (Figure 5a, nm silica). Interestingly, this effect only applies to nanoparticle-coated liquid marbles; for those coated with microparticles, the increment in conductivity tends to have a negligible impact (Figure 5a, 6 μm silicone resin).

A likely mechanism to explain the effect of electrical conductivity on U_c is the responsive capacitance from the electric double-layer (EDL) on the particle shell surface when a liquid marble is exposed to an electric field. The structure of the induced double-layer is shown in Figure 5b. As concentrated electrolyte dissolves in the droplet, by assuming there is no voltage difference across the droplet, the corresponding model for the liquid marble is proposed in Figure S5. The equivalent capacitance C_{P1}' would be the sum of electrical double-layer capacitance C_{EDL} cascaded with the capacitance of the particle shell C_{P1} that contacts the dielectric. The equivalent capacitance C_{P1}' reads

$$C_{P1}' = C_{P1} \frac{1}{\frac{C_{P1}}{C_{EDL}} + 1} \quad (1)$$

To explain the unexpected tendency qualitatively, we apply the widely accepted Gouy-Chapman-Stern (GCS) model.⁴¹ The GCS model characterizes the EDL as a Stern layer with a finite thickness and a diffuse layer with Debye length λ_D . The thickness of the Stern layer at a charged interface would be compressed and respond with a higher capacitance when the electrolyte concentration is increased.⁴¹ A similar situation also applies to the diffuse layer with thickness $\lambda_{diff} \sim \lambda_D$. Therefore, the effective double layer becomes thinner at higher electrolyte concentration and induces a larger capacitance C_{EDL} . By assuming the capacitance of the particle shell is unchanged, the cascaded capacitance C_{P1}' would increase accordingly. Referring to eqn. (6) in Supporting Information, we could derive an increment in the capacitive voltage dividing parameter β , which indicates that a smaller U_c is needed to reach the critical E_{loc} to overcome the restoring capillary pressure. This agrees well with the trend observed in our experiments.

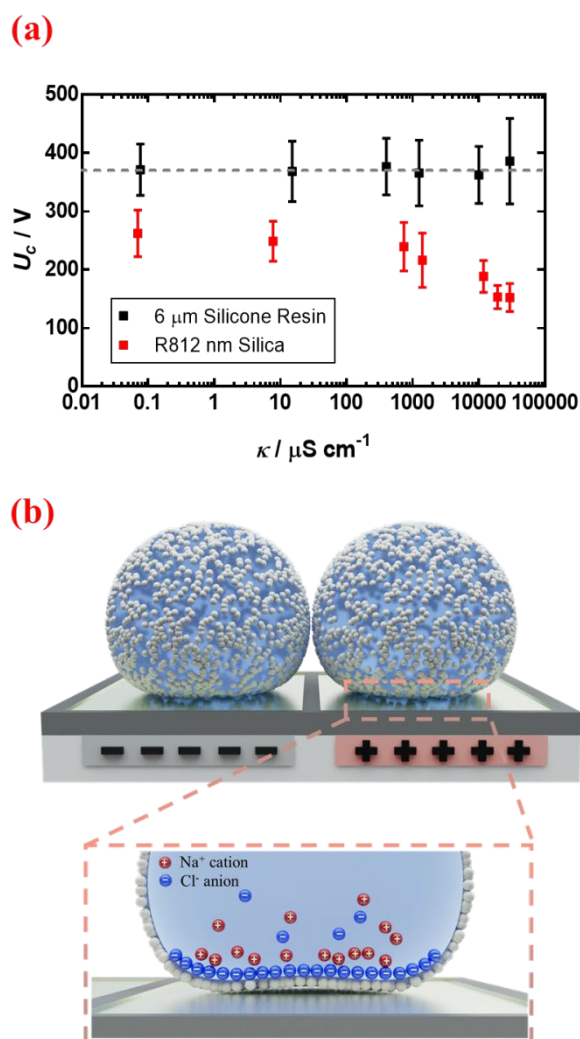


Figure 5. (a) Linear-log plot showing the dependence of critical voltage U_c on electrical conductivity κ for both silica nanoparticle and silicone resin microparticle-coated liquid marbles. (b) Schematic shows the double layer formed at the boundary of particles. The double-layer capacitance is formed due to the high electrical conductivity of the encapsulated droplet.

Therefore, this electric double-layer capacitance only takes effect when the particle layer is thin. As for nanoparticle-coated liquid marbles, the primary diameter of silica nanoparticles is 7 nm and a few hundred nanometers for particle aggregates, the specific capacitance of the particle shell would be around $\sim 10^{-5} \text{ F m}^{-2}$. The resultant capacitance of the particle layer for microparticle-based liquid marbles drops to $\sim 10^{-6} \text{ F m}^{-2}$. As no obvious influence towards the critical voltage is observed, the equivalent capacitance C_{P1}' for microparticle-based liquid marbles is not expected to differ significantly from the original C_{P1} . The value of the electric double-layer capacitance C_{EDL} is expected to be within the range of 10^{-6} F m^{-2} and 10^{-5} F m^{-2} .

3.3. Biomedical applications in liquid marbles triggered by electrocoalescence

Liquid marbles acting as micro-reactors have great potential for applications. To realize the promise, robust and efficient methodologies to coalesce and trigger the proposed micro-reactions without agitating the encapsulated droplets is critical. In our previous

work, charging the encapsulated droplets can trigger coalescence³² but the requirement of direct immersion of electrodes into the marbles also limits its applicability to viscous glycerol solution-containing chemical reactions.³³

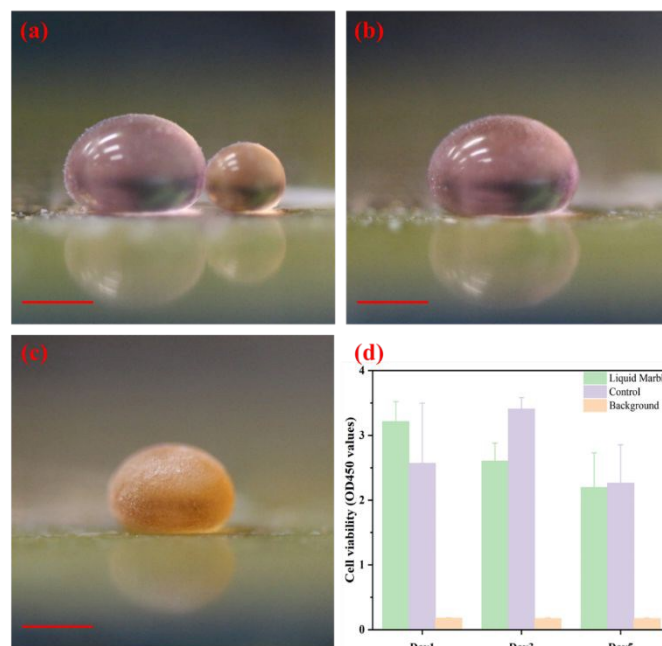


Figure 6. (a) Two liquid marbles (50 μL and 10 μL respectively) containing hBMSCs in culture medium (left) or WST-8 (CCK-8 reagents, right) before electrocoalescence. (b) Merged spherical marble of (a) with a volume of 60 μL after electrocoalescence. (c) Same marble as in (b) after being incubated at 37 $^{\circ}\text{C}$, 5% CO_2 atmosphere for 3 h; the shrinkage in size is attributed to evaporation under elevated temperature. All scale bars = 2 mm. (d) Intensity of CCK-8 of hBMSCs cultured in liquid marble micro-bioreactors, 96 well microplates (Control) and bulk culture medium without cells (background) on day 1, 3 and 5. Each bar from the above histogram comes from averaging at least four independent samples.

It should be noted that cell lysis would still be induced if the electrostatic field applied is sufficiently high.^{42, 43} However, electrocoalescence driven by embedded electrodes can avoid the electrolysis problem which often interferes with the target reactions, for instance, to assay cell viability. As a demonstration, two liquid marbles containing either human bone mesenchymal stem cells (hBMSCs) or CCK-8 reagent water-soluble tetrazolium salt (WST-8) with a volume of 50 μL and 10 μL , respectively, are prepared as shown in Figure 6a. By increasing the voltage to a critical value, the liquid marbles coalesce (Figure 6b). After incubation for three hours, the colour change in the coalesced marble suggests that cells remain alive after the electrostatics-driven coalescence (Figure 6c). Quantitative data of cell viability shows no significant difference in cell viability after five days of culture of cells in a liquid marble micro-reactor and in the traditional 2D microplate (Figure 6d). The electrostatics-driven approach also shows no effect towards the morphology of cell aggregation structures throughout the process, as indicated by the formation of a spheroid after culturing in a liquid marble micro-reactor (Figure S6).

Overall, the immersion-free electrocoalescence provides a promising strategy for studying the physical/chemical processes in liquid marbles. The ability to address individual liquid marbles without immersing electrodes in them extend the potential of existing applications towards digital liquid-marble-based

microfluidics.⁴⁴⁻⁴⁶ Moreover, it represents an important advance that allows more sophisticated chemical or biochemical reactions triggered by merging of multiple liquid marbles containing different reagents. Our results also confirm that electrocoalescence-based manipulation is compatible with cell studies, highlighting its suitability for bioreactions in liquid marble micro-reactors.

Conclusions

In this study, we have developed a robust method to coalesce liquid marbles in an immersion-free, electro-driven approach. We have overcome the need to immerse electrodes into the marbles. By utilizing electrostatics applied on embedded electrodes coated with a dielectric, two liquid marbles can coalesce when a critical voltage is applied. Based on liquid marbles coated with nanoparticles, electrocoalescence can be reliably induced by applying a voltage to overcome the capillary pressure by an electric stress. The electrical conductivity of the encapsulated droplet, which is often believed to have no impact, is also observed to affect the critical voltage. We attribute this phenomenon to the non-negligible double-layer capacitance induced from the highly concentrated electrolyte under an electric field. Finally, we confirm the potential to trigger micro-reactions in liquid marbles using our immersion-free electrocoalescence approach by measuring cell metabolic activities. Our understanding of electrocoalescence of liquid marbles *via* embedded electrodes on a dielectric is essential for manipulating large numbers of liquid marble micro-reactors for chemical and biological assays in an automated manner.

Author contributions

Y. Zhang and X. Fu proposed the idea. Y. Zhang developed and conducted the majority of the experiments and prepared the original draft. Y. Zhang and W. Guo created the model. Y. Deng helped with the biomedical investigation. B. P. Binks and H. C. Shum reviewed and edited the original draft. H. C. Shum supervised the project. All authors read and approved the final manuscript.

Conflicts of interest

The authors state that there are no conflicts to declare.

Acknowledgements

We thank Prof. Huisheng Zhang, Dr. Zhou Liu, Dr. Tiantian Kong and Dr. Yuan Liu for helpful discussions. We thank Mr. Hao Lyv for providing human mesenchymal stem cells. This research was supported by the General Research Fund (Nos. 17304514, 17306315, 17304017 and 17329516) from the Research Grants Council of Hong Kong, Seed Fund for Basic Research (Nos. 201711159249, 201611159205 and 201511159280), Seed Fund for Translational and Applied Research (No. 201711160016) from the University of Hong Kong and Sichuan Science and Technology Program (2018JZ0026).

References

- G. M. Whitesides, *Nature*, 2006, **442**, 368-373.
- K. Choi, A. H. Ng, R. Fobel and A. R. Wheeler, *Annu. Rev. Anal. Chem.* 2012, **5**, 413-440.
- D. R. Link, E. Grasland-Mongrain, A. Duri, F. Sarrazin, Z. Cheng, G. Cristobal, M. Marquez and D. A. Weitz, *Angew. Chem. Int. Ed.*, 2006, **45**, 2556-2560.
- P. Aussillous and D. Quéré, *Nature*, 2001, **411**, 924-927.
- M. Dandan and H. Y. Erbil, *Langmuir*, 2009, **25**, 8362-8367.
- C. Fullarton, T. C. Draper, N. Phillips, R. Mayne, B. P. J. de Lacy Costello and A. Adamatzky, *Langmuir*, 2018, **34**, 2573-2580.
- Z. Liu, Y. Zhang, C. Chen, T. Yang, J. Wang, L. Guo, P. Liu and T. Kong, *Small*, 2018, **15**, 1804549.
- Y. Sheng, G. Sun, J. Wu, G. Ma and T. Ngai, *Angew. Chem. Int. Ed.*, 2015, **54**, 7012-7017.
- Y. E. Miao, H. K. Lee, W. S. Chew, I. Y. Phang, T. Liu and X. Y. Ling, *Chem. Commun.*, 2014, **50**, 5923-5926.
- W. Gao, H. K. Lee, J. Hobley, T. Liu, I. Y. Phang and X. Y. Ling, *Angew. Chem. Int. Ed.*, 2015, **54**, 3993-3996.
- D. Wang, L. Zhu, J. F. Chen and L. Dai, *Angew. Chem. Int. Ed.*, 2016, **55**, 10795-10799.
- T. Arbatan, L. Li, J. Tian and W. Shen, *Adv. Healthc. Mater.*, 2012, **1**, 80-83.
- E. Bormashenko and A. Musin, *Appl. Surf. Sci.*, 2009, **255** (12), 6429-6431.
- J. Tian, T. Arbatan, X. Li and W. Shen, *Chem. Commun.*, 2010, **46**, 4734-4736.
- J. Tian, T. Arbatan, X. Li and W. Shen, *Chem. Eng. J.*, 2010, **165**, 347-353.
- M. Paven, H. Mayama, T. Sekido, H. J. Butt, Y. Nakamura and S. Fujii, *Adv. Funct. Mater.*, 2016, **26**, 3199-3206.
- H. Kawashima, M. Paven, H. Mayama, H. J. Butt, Y. Nakamura and S. Fujii, *ACS Appl. Mater. Interfaces*, 2017, **9** (38), 33351-33359.
- T. Arbatan, A. Al-Abboodi, F. Sarvi, P. P. Chan and W. Shen, *Adv. Healthc. Mater.*, 2012, **1**, 467-469.
- R. K. Vadivelu, C. H. Ooi, R.-Q. Yao, J. Tello Velasquez, E. Pastrana, J. Diaz-Nido, F. Lim, J. A. Ekberg, N. T. Nguyen and J. A. St John, *Sci. Rep.*, 2015, **5**, 15083.
- R. K. Vadivelu, H. Kamble, A. Munaz and N. T. Nguyen, *Sci. Rep.*, 2017, **7**, 12388.
- H. Li, P. Liu, G. Kaur, X. Yao and M. Yang, *Adv. Healthc. Mater.*, 2017, **6**, 1700185.
- J. Jin, C. H. Ooi, D. V. Dao and N. T. Nguyen, *Micromachines*, 2017, **8**, 336.
- J. Jin, C. H. Ooi, D. V. Dao and N. T. Nguyen, *Soft Matter*, 2018, **14**, 4160-4168.
- C. Planchette, A.-L. Biance, O. Pitois and E. Lorenceau, *Phys. Fluids*, 2013, **25**, 042104.
- T. C. Draper, C. Fullarton, R. Mayne, N. Phillips, G. E. Canciani, B. P. J. de Lacy Costello and A. Adamatzky, *Soft Matter*, 2019, **15**, 3541-3551.
- D. Zang, J. Li, Z. Chen, Z. Zhai, X. Geng and B. P. Binks, *Langmuir*, 2015, **31**, 11502-11507.
- Z. Chen, D. Zang, L. Zhao, M. Qu, X. Li, X. Li, L. Li and X. Geng, *Langmuir*, 2017, **33**, 6232-6239.
- Y. Zhao, J. Fang, H. Wang, X. Wang and T. Lin, *Adv. Mater.*, 2010, **22**, 707-710.
- L. Zhang, D. Cha and P. Wang, *Adv. Mater.*, 2012, **24**, 4756-4760.
- Y. Zhao, Z. Xu, H. Niu, X. Wang and T. Lin, *Adv. Funct. Mater.*, 2015, **25**, 437-444.
- Y. Zhao, H. Gu, Z. Xie, H. C. Shum, B. Wang and Z. Gu, *J. Am. Chem. Soc.*, 2013, **135**, 54-57.
- Z. Liu, X. Fu, B. P. Binks and H. C. Shum, *Soft Matter*, 2016, **13**, 119-124.

ARTICLE

Journal Name

- 33 Z. Liu, T. Yang, Y. Huang, Y. Liu, L. Chen, L. Deng, H. C. Shum and T. Kong, *Adv. Funct. Mater.*, 2019, **29**, 1901101.
- 34 B. Song and J. Springer, *J. Colloid Interface Sci.* 1996, **184**, 64-76.
- 35 B. Song and J. Springer, *J. Colloid Interface Sci.* 1996, **184**, 77-91.
- 36 D. G. A. L. Aarts, H. N. W. Lekkerkerker, H. Guo, G. H. Wegdam and D. Bonn, *Phys. Rev. Lett.* 2005, **95**, 164503.
- 37 Y. Nam, H. Kim and S. Shin, *Appl. Phys. Lett.* 2013, **103**, 161601.
- 38 E. Bormashenko, Y. Bormashenko, R. Pogreb and O. Gendelman, *Langmuir*, 2011, **27**, 7-10.
- 39 C.-C. Chang, C.-J. Wu, Y.-J. Sheng and H.-K. Tsao, *Soft Matter*, 2015, **11**, 4469-4475.
- 40 G. Chen, P. Tan, S. Chen, J. Huang, W. Wen and L. Xu, *Phys. Rev. Lett.* 2013, **110**, 064502.
- 41 M. A. Brown, A. Goel and Z. Abbas, *Angew. Chem. Int. Ed.*, 2016, **55**, 3790-3794.
- 42 H.-Y. Wang and C. Lu, *Chem. Commun.*, 2006, 3528-3530.
- 43 H.-Y. Wang, A. K. Bhunia and C. Lu, *Biosens. Bioelectron.*, 2006, **22**, 582-588.
- 44 X. Fu, Y. Zhang, H. Yuan, B. P. Binks and H. C. Shum, *ACS Appl. Mater. Interfaces*, 2018, **10**, 34822-34827.
- 45 M. I. Newton, D. L. Herbertson, S. J. Elliott, N. J. Shirtcliffe and G. McHale, *J. Phys. D: Appl. Phys.*, 2007, **40**, 20-24.
- 46 G. McHale, D. L. Herbertson, S. J. Elliott, N. J. Shirtcliffe and M. I. Newton, *Langmuir*, 2007, **23**, 918-924.

View Article Online
DOI: 10.1039/C9LC00722A

We present coalescence of liquid marbles in a non-contact approach by applying electrostatics to embedded electrodes.

